NASA Technical Memorandum 110223

# A Preliminary Study of a Wake Vortex Encounter Hazard Boundary for a B737-100 Airplane

Heidi M. Reimer and Dan D. Vicroy
*Langley Research Center, Hampton, Virginia*

April 1996

National Aeronautics and
Space Administration
Langley Research Center
Hampton, Virginia 23681-0001

# A Preliminary Study of a Wake Vortex Encounter Hazard Boundary for a B737-100 Airplane


## Abstract

A preliminary batch simulation study was conducted to define the wake decay required for a Boeing 737-100 airplane to safely encounter a Boeing 727 wake and land. The baseline six-degree-of-freedom B737 simulation was modified to include a wake model and the strip-theory calculation of the vortex-induced forces and moments. The guidance and control inputs for the airplane were provided by an autoland system. The wake strength and encounter altitude were varied to establish a safe encounter boundary. The wake was positioned such that the desired flight path traversed the core of the port vortex. Various safe landing criteria were evaluated for defining a safe encounter boundary. A sensitivity study was also conducted to assess the effects of encounter model inaccuracies.


## Introduction

Many of today's major airports are capacity limited, leading to increased airport congestion and delays. With air-traffic continuing to increase and very few new airports being built, this trend is expected to continue. The National Aeronautics and Space Administration (NASA), the Federal Aviation Administration (FAA), airport operators, and the airline industries are all interested in methods to improve airport capacity. One way to improve capacity is to reduce the in-trail spacing of airplanes.

One of the limiting factors on reducing airplane separations is the spacing required to avoid the wake turbulence of the preceding airplane. Wake turbulence is primarily formed from vortices shed from the wing of the leading airplane. Wake vortices are horizontally oriented, counter-rotating "mini-tornadoes," separated by slightly less than the span of the generating wing. Vortex encounters are particularly hazardous during landings and takeoffs. An aircraft encountering one of these vortices could be mildly disturbed or catastrophically upset. The degree of upset depends mainly on the relative size of the vortex generating and vortex penetrating airplane. The vortex initial energy or strength and the resulting response to the wake are directly related to aircraft size and weight. The probability of encountering the wake of a preceding airplane is reduced as longitudinal spacing between the aircraft pair is increased. The increased spacing provides time for the decay and transport of the vortex pair out of the flight path of the trailing airplane.

Currently, there are spacing intervals mandated for operations under instrument flight rules (IFR) by the Federal Aviation Administration (FAA). These intervals (Table 1) range from three to six miles and are a function of the takeoff gross weight of the leading and trailing aircraft. Aircraft are classified as Heavy (300,000 lb or more), Large (between 12,500 and 300,000 lb), or Small (less than 12,500 lb).

| Following Aircraft | Leading Aircraft | | |
|---|---|---|---|
| | Heavy | Large | Small |
| Heavy | 4 | 3 | 3 |
| Large | 5 | 3 | 3 |
| Small | 6 | 4 | 3 |

Table 1 - U.S. wake vortex separation standards, distances in nautical miles.

During operations under visual flight rules (VFR), the pilot is normally requested to visually maintain safe separation with the preceding airplane. Under these circumstances, pilots tend to fly with less separation than required under IFR operations. The difference between the IFR separation requirements and the reduced yet apparently safe VFR separations, have led researchers to believe that the IFR regulations may be unnecessarily conservative. If IFR separations are too conservative then it follows that airport capacities could be increased by safely reducing the separation standards.

The NASA began the Terminal Area Productivity (TAP) Program to provide the technology required to enable safe improvements in airport capacity. The TAP Program consists of four elements: Air Traffic Management, Aircraft-Air Traffic Control Systems Integration, Low-Visibility Landing and Surface Operations, and Reduced Spacing Operations. The work described within this paper falls under the Reduced Spacing Operations element.

There are several areas of research required to safely reduce separation requirements. This research includes vortex motion and decay prediction, vortex encounter modeling, wake-vortex hazard characterization, and vortex detection. This paper describes a simulation study that is part of the hazard characterization research. This preliminary simulation study tested various safe landing criteria to define the wake decay required for a Boeing 737-100 airplane to safely encounter a Boeing 727 wake and land. The wake strength and encounter altitude were varied to establish a safe encounter boundary. A sensitivity study was also conducted to assess the effects of model inaccuracies.

Symbols

| | |
|---|---|
| $b$ | wing span, ft |
| $\bar{c}$ | mean aerodynamic chord, ft |
| $C_l$ | rolling moment coefficient |
| $c_{\ell_\alpha}$ | 2-dimensional lift curve slope, $\partial c_\ell / \partial \alpha$ |
| $C_L$ | lift coefficient |
| $C_m$ | pitching moment coefficient |
| $C_n$ | yawing moment coefficient |
| $C_Y$ | sideforce coefficient |
| $h_v$ | altitude of vortex pair above the runway, ft |
| $N_{strips}$ | total number of strips |
| $r_c$ | vortex core radius, ft |
| $r$ | radius from vortex center, ft |
| $S$ | planform reference area, ft$^2$ |
| $S_i$ | reference area of strip $i$, ft$^2$ |
| $v$ | velocity component along $Y$ axis, ft/s |
| $V_\theta$ | vortex tangential velocity, ft/s |
| $w$ | velocity component along $Z$ axis, ft/s |
| $y$ | coordinate along $Y$ axis, ft |
| $Y$ | lateral axis |
| $z$ | coordinate along Z axis, ft |
| $Z$ | vertical axis |
| $\alpha_N$ | angle of attack in a plane normal to the planform, rad |
| $\alpha_s$ | strip angle of incidence, rad. |
| $\delta$ | dihedral angle, rad |
| $\theta$ | pitch angle, rad |
| $\phi$ | roll angle, rad |
| $\psi$ | yaw angle, rad |
| $\Gamma$ | vortex circulation strength, ft$^2$/s |

Subscripts

| | |
|---|---|
| $b$ | reference to body axis system |
| $c/4$ | reference to strip 1/4 chord point |
| $i$ | reference to strip $i$ |
| $I$ | reference to inertial axis system |
| $L$ | reference to left or port vortex |
| $p$ | reference to point P |

| | |
|---|---|
| *rwy* | reference to runway axis system |
| *R* | reference to right or starboard vortex |
| *w* | wake-induced component |
| $\infty$ | free-stream component |

Previous Vortex Encounter Simulations

A number of vortex-encounter simulations were performed during the 1970s and 1980s. Among these, three studies stand out as particularly relevant to this simulation. In 1974, Nelson and McCormick (refs 1, 2, 3) studied vortex encounters with a batch simulation using analytical transfer functions to represent the pilot. Sammonds, Stinnet, and Larson (refs 4, 5, 6) used a piloted wake encounter simulation to establish hazard criteria from pilot opinion. Hastings and Keyser (ref 7) studied the effect of vortex decay on the initial response of a twin-engine transport airplane with a piloted simulation. Each of these simulation studies used strip theory to model the vortex effect on the airplane. The same method was used in this study and will be discussed later. These simulations differed from this study in that they were primarily focused on defining what constitutes a hazardous wake encounter. This study is interested in what constitutes an acceptable and safe wake encounter. In particular, the encounter must be weak enough that the airplane can continue the approach and landing without undue upsets to the passengers and crew.

B737-100 Wake Encounter Simulation

The baseline B737-100 simulation was a batch version of the six-degree-of-freedom real-time simulation of NASA Langley's Advanced Transport Operating System research airplane shown in figure 1. This simulation was also used in Hastings' vortex encounter study (ref 7). The baseline simulation was modified to include the wake model and the strip-theory calculation of the vortex-induced forces and moments. Instead of using a pilot model, the control inputs were generated by an automatic landing system.

The geometry of the encounter simulation is shown in sketch A. The airplane was initially trimmed for a 3° glideslope approach to landing. It began 24,000 feet out from the runway threshold, at an altitude of 1,323 feet, and was correctly centered on the localizer and glideslope. A pair of vortices stretched from 24,300 feet before the runway threshold to 10,000 feet after the threshold. The airplane encountered the core of the port vortex at a predefined altitude ($h_v$).

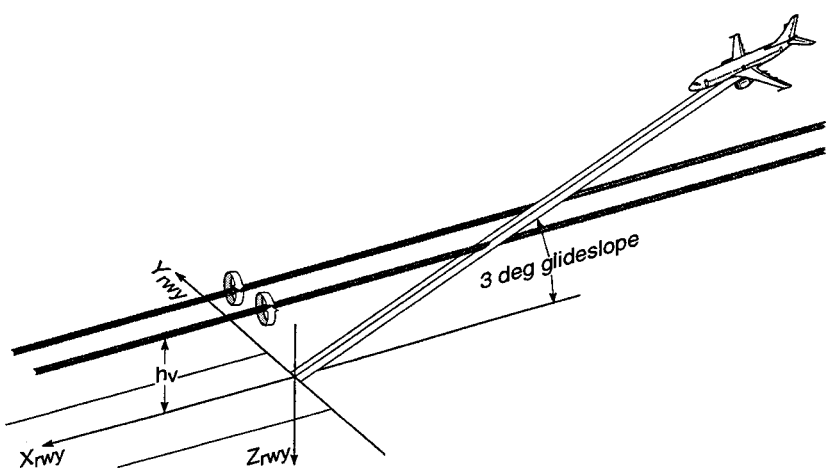


**Sketch A. Wake encounter simulation geometry.**

Simulation calculations were performed at a rate of 32 iterations per second, and the output data was recorded once per second. At each sample interval, 25 variables were recorded. These variables included:

- Aircraft position relative to the runway axis system
- Aircraft attitude, rotational rates, and flight path
- Aerodynamic coefficients due to the vortex
- Control surface positions

These data were analyzed to determine the maximum and minimum of selected variables along with specified conditions at touchdown.

Vortex Model

An empirically derived two-dimensional wake vortex model was used to describe the wake of the generating wing. This wake model was proposed by Burnham in reference 8 to fit field measurement data of airplane wakes. The model is defined in the inertial axis system by the circulation ($\Gamma$), core radius $(r_c)$ and location $(y, z)$ of two counter-rotating vortices, as shown in sketch B.

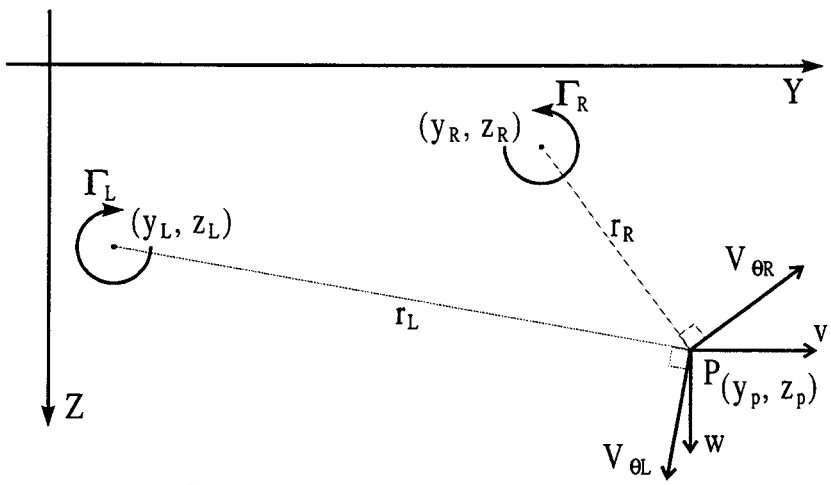


**Sketch B. Two-dimensional wake model.**

The Burnham model defines the tangential velocity ($V_\theta$) of a single vortex as:

$$V_\theta = \frac{\Gamma}{2\pi}\left(\frac{r}{r_c^{\,2} + r^2}\right) \tag{1}$$

where $r$ is the radius from the center of the vortex. The sidewash $(v)$ and downwash $(w)$ velocity components at a point P are obtained by summing the contributions of the left and right vortices. The contributions from the left vortex are:

$$v_L = V_{\theta L}\frac{z_L - z_p}{r_L} = \frac{\Gamma_L}{2\pi}\left(\frac{z_L - z_p}{r_{c_L}^{\,2} + r_L^{\,2}}\right) \tag{2}$$

and

$$w_L = V_{\theta L}\frac{y_p - y_L}{r_L} = \frac{\Gamma_L}{2\pi}\left(\frac{y_p - y_L}{r_{c_L}^{\,2} + r_L^{\,2}}\right) \tag{3}$$

where

$$r_L = \sqrt{\left(y_p - y_L\right)^2 + \left(z_p - z_L\right)^2} \tag{4}$$

The corresponding contributions from the right vortex are:

$$v_R = V_{\theta R}\frac{z_p - z_R}{r_R} = \frac{\Gamma_R}{2\pi}\left(\frac{z_p - z_R}{r_{c_R}{}^2 + r_R{}^2}\right) \tag{5}$$

and

$$w_R = V_{\theta R}\frac{y_R - y_p}{r_R} = \frac{\Gamma_R}{2\pi}\left(\frac{y_R - y_p}{r_{c_R}{}^2 + r_R{}^2}\right) \tag{6}$$

where

$$r_R = \sqrt{\left(y_p - y_R\right)^2 + \left(z_p - z_R\right)^2} \tag{7}$$

Summing the contributions of the left and right vortices yields the sidewash and downwash velocities at the point P.

$$v = v_L + v_R = \frac{1}{2\pi}\left[\Gamma_R\left(\frac{z_p - z_R}{r_{c_R}{}^2 + r_R{}^2}\right) - \Gamma_L\left(\frac{z_p - z_L}{r_{c_L}{}^2 + r_L{}^2}\right)\right] \tag{8}$$

$$w = w_L + w_R = \frac{1}{2\pi}\left[\Gamma_L\left(\frac{y_p - y_L}{r_{c_L}{}^2 + r_L{}^2}\right) - \Gamma_R\left(\frac{y_p - y_R}{r_{c_R}{}^2 + r_R{}^2}\right)\right] \tag{9}$$

For this simulation study the wake model variables were set to represent the wake of a B727 size airplane. The core radius for both vortices was set at 2 feet ($r_{c_L} = r_{c_R} = 2$). The circulation and altitude of the vortices were varied throughout the study, but were constrained to be symmetrical ($z_L = z_R$, $\Gamma_L = \Gamma_R$). The left vortex was placed in line with the runway centerline ($y_L = 0$) with the right vortex spaced 84 feet to the side ($y_R = 84$).

Vortex Encounter Aerodynamics

The aerodynamic effect of the wake on the encountering airplane was modeled using a strip theory method similar to that used in references 4, 5 and 6. Strip theory is a simple method in which the wing, the horizontal stabilizer and the vertical stabilizer are divided into a series of chordwise strips, as shown in sketch C. Each strip is treated as a 2-dimensional airfoil for which the lift at the quarter-chord point is computed as a function of the flow incidence angle at the three-quarter-chord point. The incremental contribution of each strip is summed to determine the forces and moments on the airplane.

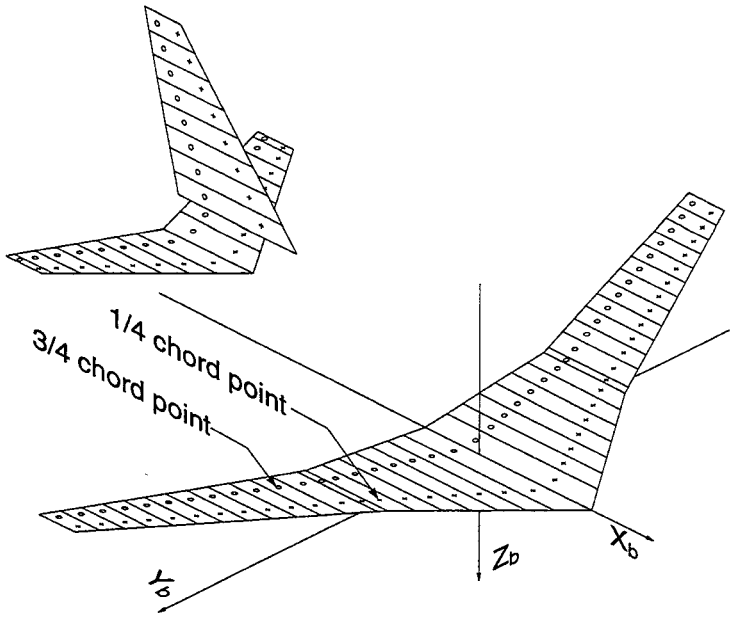


**Sketch C. Strip model of B737-100.**

Each strip is defined by its area, 2-dimensional lift-curve slope, angle of incidence, dihedral angle, and the body axis coordinates of the quarter and three-quarter points at the mid-span of the strip. The lift-curve slope of each strip was weighted to yield the proper span load distribution in a uniform flow field.

The force and moment contributions from each strip were determined in the following manner. First the free-stream and wake-induced velocities at the strip three-quarter-chord point are translated from the inertial-axis system to the body-axes system through:

$$\begin{pmatrix} u_b \\ v_b \\ w_b \end{pmatrix} = \begin{pmatrix} \cos\theta\cos\psi & \cos\theta\sin\psi & -\sin\theta \\ \sin\phi\sin\theta\cos\psi - \sin\psi\cos\phi & \sin\psi\sin\theta\sin\phi + \cos\psi\cos\phi & \sin\phi\cos\theta \\ \cos\psi\cos\phi\sin\theta + \sin\psi\sin\phi & \sin\psi\cos\phi\sin\theta - \cos\psi\sin\phi & \cos\phi\cos\theta \end{pmatrix} \begin{pmatrix} u_I \\ v_I \\ w_I \end{pmatrix} \tag{10}$$

The free-steam and wake velocities are then summed to yield the local body-axes velocities for the strip $i$.

$$\begin{aligned} u_i &= u_\infty + u_{w_i} \\ v_i &= v_\infty + v_{w_i} \\ w_i &= w_\infty + w_{w_i} \end{aligned} \tag{11}$$

The strip angle of attack in a plane normal to the planform was then computed from:

$$\alpha_{N_i} = \alpha_{s_i} + \tan^{-1}\left( \frac{w_i \cos\delta_i - v_i \sin\delta_i}{u_i} \right) \tag{12}$$

for planforms on the right half of the airplane, and:

$$\alpha_{N_i} = \alpha_{s_i} + \tan^{-1}\left(\frac{w_i \cos\delta_i + v_i \sin\delta_i}{u_i}\right) \tag{13}$$

for planforms on the left half of the airplane.

For vertical surfaces the dihedral angle is 90° and the angle of attack normal to the planform is approximately the negative of the local sideslip angle.

The lift coefficient for the strip was computed from:

$$C_{L_i} = \frac{S_i}{S} c_{\ell_i} \alpha_{N_i} \cos\delta_i \tag{14}$$

The corresponding sideforce coefficient was:

$$C_{Y_i} = \frac{S_i}{S} c_{\ell_i} \alpha_{N_i} \sin\delta_i \tag{15}$$

The drag coefficient term was neglected with this method.

The total force and moment coefficients were determined by summing the contributions of each strip.

$$C_L = \sum_{i=1}^{N_{strips}} C_{L_i} \tag{16}$$

$$C_Y = \sum_{i=1}^{N_{strips}} C_{Y_i} \tag{17}$$

$$C_l = -\frac{1}{b} \sum_{i=1}^{N_{strips}} \left( C_{L_i} y_{c/4_i} + C_{Y_i} z_{c/4_i} \right) \tag{18}$$

$$C_m = \frac{1}{\bar{c}} \sum_{i=1}^{N_{strips}} C_{L_i} x_{c/4_i} \tag{19}$$

$$C_n = \frac{1}{b} \sum_{i=1}^{N_{strips}} C_{Y_i} x_{c/4_i} \tag{20}$$

The change in the aerodynamic forces and moments due to the wake was determined by taking the difference between the strip theory calculation with the wake velocities included and the same calculation with the wake velocities set to zero. For example:

$$\Delta C_{L_w} = C_{L_{\text{wake}}} - C_{L_{\text{no wake}}} \tag{21}$$

The change in the force and moment coefficients due to the wake were then added to the baseline six-degree-of-freedom simulation coefficients.

Landing Criteria

As was discussed in the introduction, the objective of this study was to assess the wake decay required for a B737-100 to safely encounter the core of a B727 wake and land. This analysis requires the establishment of some criteria to define a safe and acceptable landing. Several metrics were examined as safe landing criteria. The most notable were maximum bank angle, lateral and vertical deviation from the flight path, and sink rate. The maximum bank angle limit was set at 10° which roughly corresponds the low-altitude hazard limit of Sammonds, Stinnet, and Larson (refs 4, 5, 6). Sink rate at touchdown was limited to four feet per second. A proposed autoland certification requirement for satellite navigation systems (ref 9) was used to define the lateral and vertical deviation limits. These limits were defined by the inner approach tunnel shown in figure 2. The tunnel dimensions are presented in table 2 as a function of altitude. The dimensions correspond to approximately a 1° localizer deviation and a 0.3° glideslope deviation. In addition to these landing criteria the maximum pitch angle, maximum yaw angle, roll rate, pitch rate, and yaw rate were also monitored.

| Altitude, ft | 0 | 50 | 100 | 200 | 250 | 300 | 400 | 500 | 750 | 1000 | 1250 | 1500 |
|---|---|---|---|---|---|---|---|---|---|---|---|---|
| Lateral, ft | ±27 | ±51 | ±75 | ±110 | ±118 | ±125 | ±158 | ±192 | ±275 | ±358 | ±442 | ±525 |
| Vertical, ft | 0 | | ±15 | ±32 | ±36 | ±40 | ±51 | ±62 | ±89 | ±116 | ±143 | ±170 |

Table 2 - Proposed flight path deviation limits for a satellite based autoland system.

The vertical path deviations were computed in a slightly different manner than the horizontal deviations. The horizontal deviations were computed relative to the localizer centerline. The vertical path deviations were computed relative to a baseline vertical profile. The profile was basically a 3° glideslope that included the flair maneuver prior to touchdown. The baseline profile was generated by recording the altitude and range for a simulation run without a wake encounter.

Simulation Analysis

Multiple wake encounter simulations were conducted with various wake strengths and altitudes. An example of the encounter simulation results are shown in figure 3 for a wake 500 feet above the runway with a circulation of 2000 $ft^2/s$. Each wake encounter was checked against the landing criteria. Of all the criteria, only maximum bank angle and lateral deviation were limiting criteria. Violations of the other limits were preceded by violations of these two criteria. Figure 4 shows the locus of maximum bank angle and lateral displacement limits as a function of wake strength and altitude. At the lower altitudes ($h_v \leq 150$ ft) the lateral deviation limit was the limiting criteria. At the higher altitudes the maximum bank angle was the predominate limiting criteria. The bank angle limit was nearly constant with altitude at a wake strength of about 2000 $ft^2/sec$.

A sensitivity study was conducted to establish error bounds for the wake encounter boundary. This analysis assessed the sensitivity of the boundary to errors in the wake encounter model. The change in the aerodynamic coefficients generated by the encounter model were multiplied by 0.9 and 1.1 to yield a ±10% error bound. The results of the modeling error on the lateral deviation boundary are shown in figure 5. The shift in the lateral deviation boundary was primarily along the wake strength axis. The -10% modeling error (90% of modeled wake effect) resulted in approximately a 11.2% increase in the acceptable wake strength. The +10% modeling error (110% of modeled wake effect) resulted in approximately a 9.1% decrease in the acceptable wake strength.

The sensitivity of the maximum bank angle boundary is shown in figure 6. The results of the bank angle sensitivity were the same as the lateral deviation results. The -10% yielded a 11.2% increase in the acceptable wake strength. The +10% modeling error resulted in a 9.2% decrease in the acceptable wake strength.

## Concluding Remarks

The results of this preliminary study indicate that above an altitude of 150 feet the maximum bank angle was the predominate limiting criteria. The bank angle criteria resulted in a wake strength boundary that was nearly constant with altitude. The lateral deviation limit was predominate for encounter altitudes at or below 150 feet and significantly decreased the acceptable wake strength boundary. For this study the vertical deviation limit was not a limiting factor. However, for wake encounters through locations other than the vortex core this may not be the case. The vertical deviation may be a limiting criterion for encounters inboard of the vortex core where the downwash of the wake is predominate.

The results of this study are the first in a planned series of studies to establish a boundary for acceptable wake encounters. Additional simulation studies will be conducted to investigate encounters through different parts of the wake and alternative methods of modeling the wake encounter. Research is also ongoing to validate the simulation encounter models with flight test and wind tunnel data.

## References


1 Nelson, R. C.: "The Response of Aircraft Encountering Aircraft Wake Turbulence," AFFDL-TR-74-29, June 1974.

2 Nelson, R. C.; and McCormick, B. W.: "The Dynamic Behavior of an Aircraft Encountering Aircraft Wake Turbulence," AIAA Paper No. 74-774, August 1974.

3 Nelson, R. C.: "Dynamic Behavior of an Aircraft Encountering Aircraft Wake Turbulence," *Journal of Aircraft*, Vol. 13, No. 9, September 1976, pp. 704-708.

4 Sammonds, R. I.; Stinnett, G. W., Jr.; and Larson, W. E.: "Hazard Criteria for Wake Vortex Encounters," NASA TM-X-62473, August 1974.

5 Sammonds, R. I.; Stinnett, G. W., Jr.; and Larson, W. E.: "Wake Vortex Encounter Hazard Criteria for Two Aircraft Classes," NASA TM-X-73113, June 1976.

6 Sammonds, R. I.; Stinnett, G. W., Jr.; and Larson, W. E.: "Criteria Relating Wake Vortex Encounter Hazard to Aircraft Response," *Journal of Aircraft*, Vol. 14, No. 10, October 1977, pp. 981-987.

7 Hastings, E. C., and Keyser, G. L., Jr.: "Simulator Study of Vortex Encounters by a Twin-Engine, Commercial, Jet Transport Airplane," NASA TP 1966, February 1982.

8 Hallock, J. N.; and Eberle, W. R.: "Aircraft Wake Vortices: A State-of-the-Art Review of the United States R&D Program," FAA-RD-77-23, February 1977.

9 Kelly, R. J.; and Davis, J. M.: "Required Navigation Performance (RNP) for Precision Approach and Landing with GNSS Application," Navigation: *Journal of The Institute of Navigation*, Vol. 41, No. 1, Spring 1994.

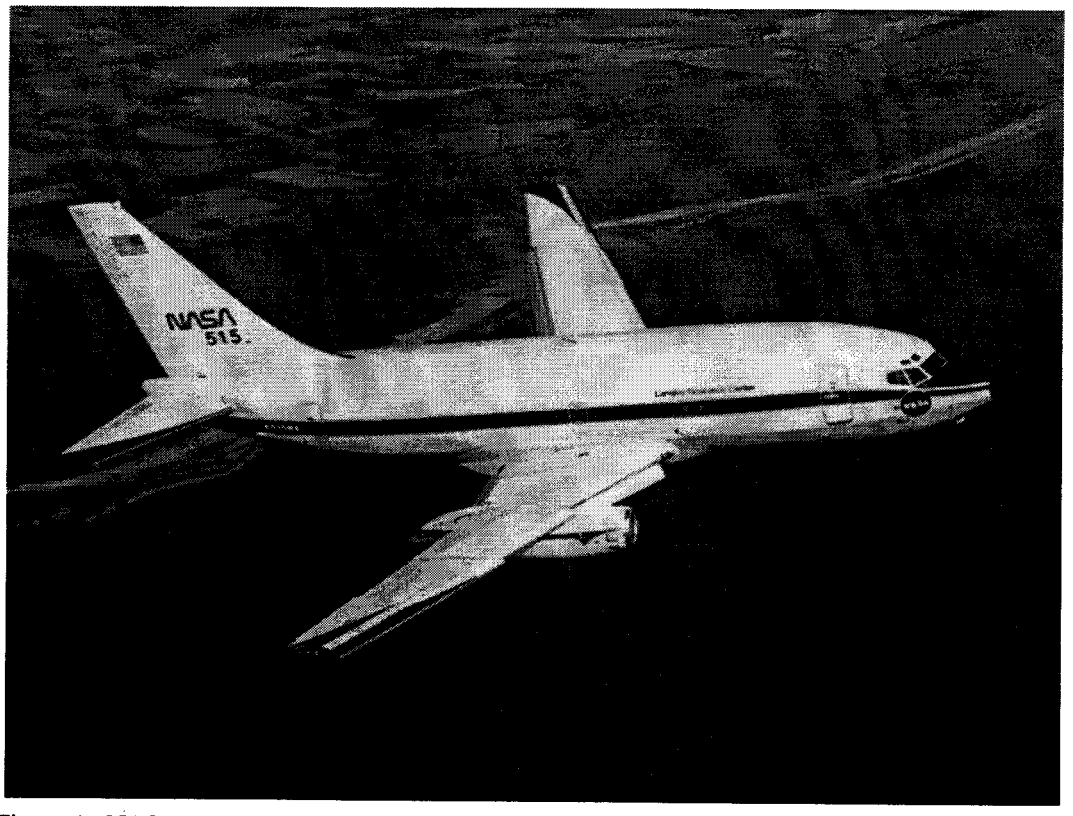


Figure 1. NASA Langley's Advanced Transport Operating System Boeing 737-100 research airplane.

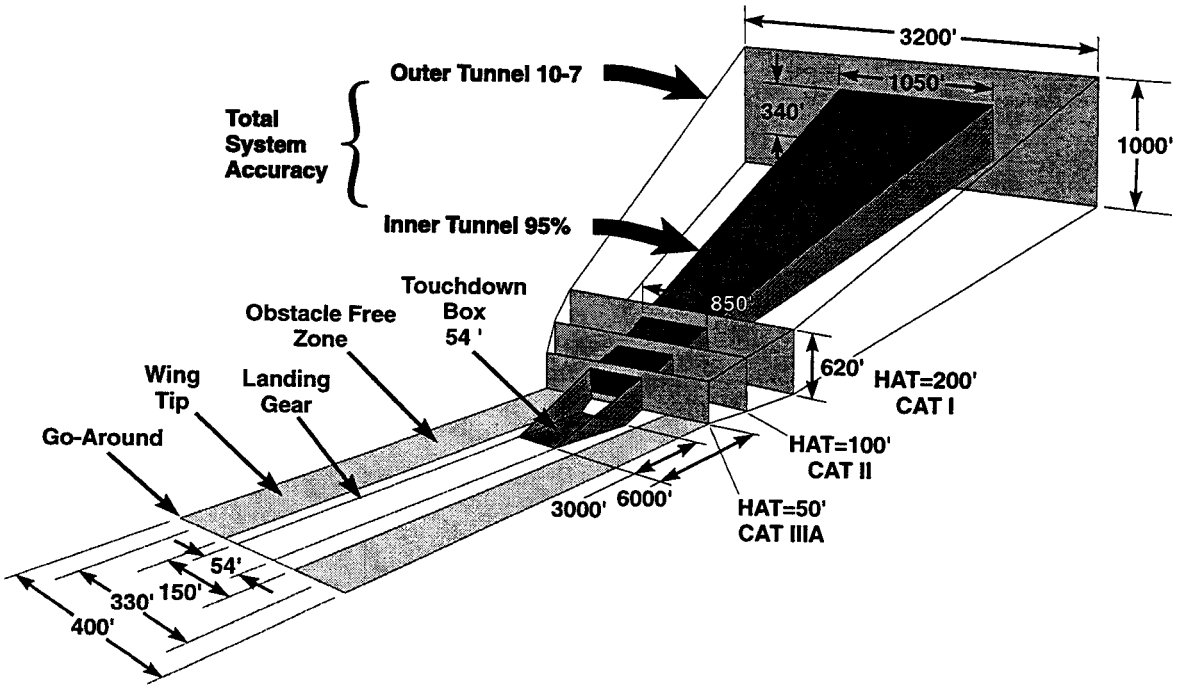


Figure 2. Proposed satellite navigation autoland certification tunnel.

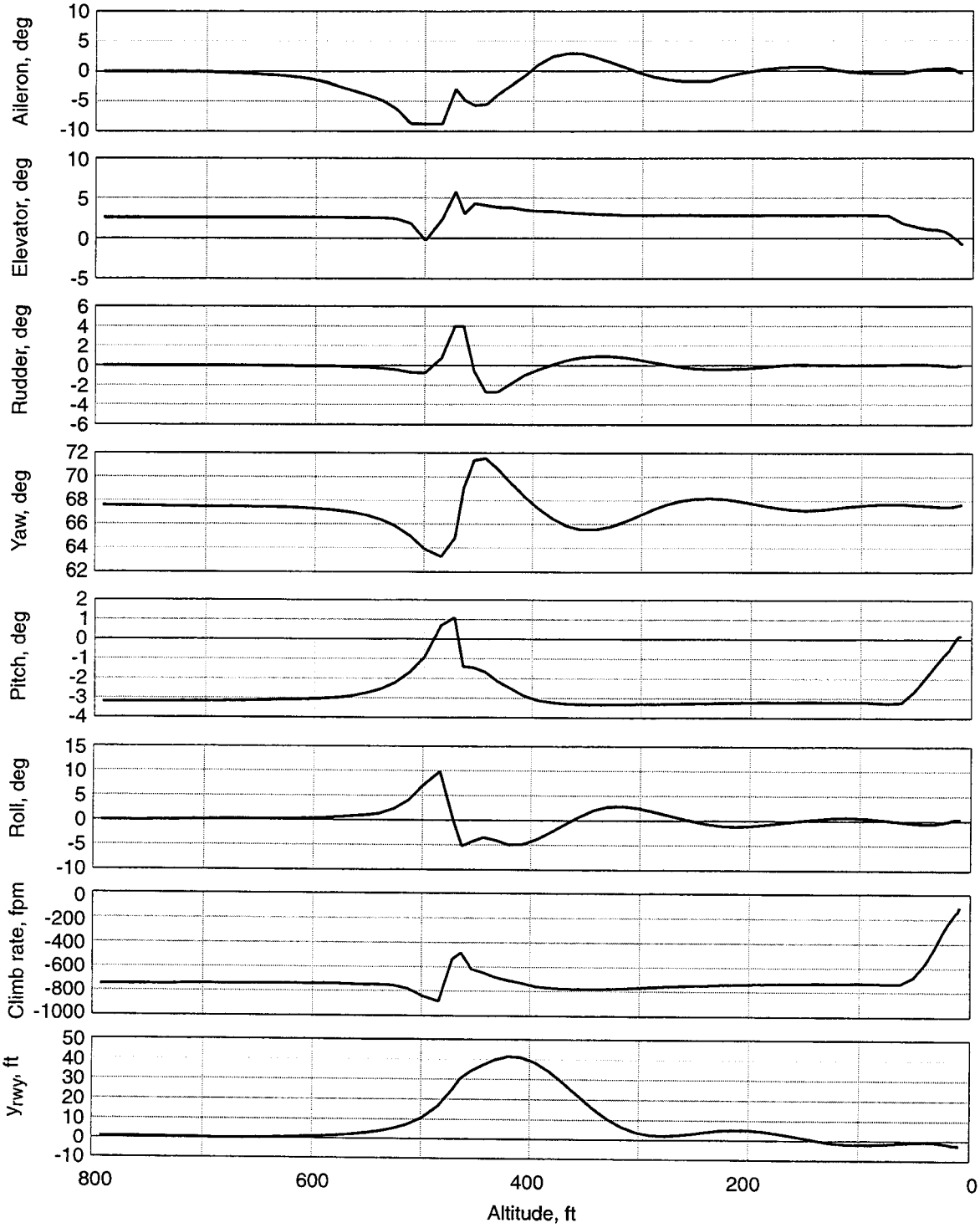


Figure 3. Simulation results of wake encounter for $h_v = 500$ ft. and $\Gamma = 2000$ ft$^2$/s.

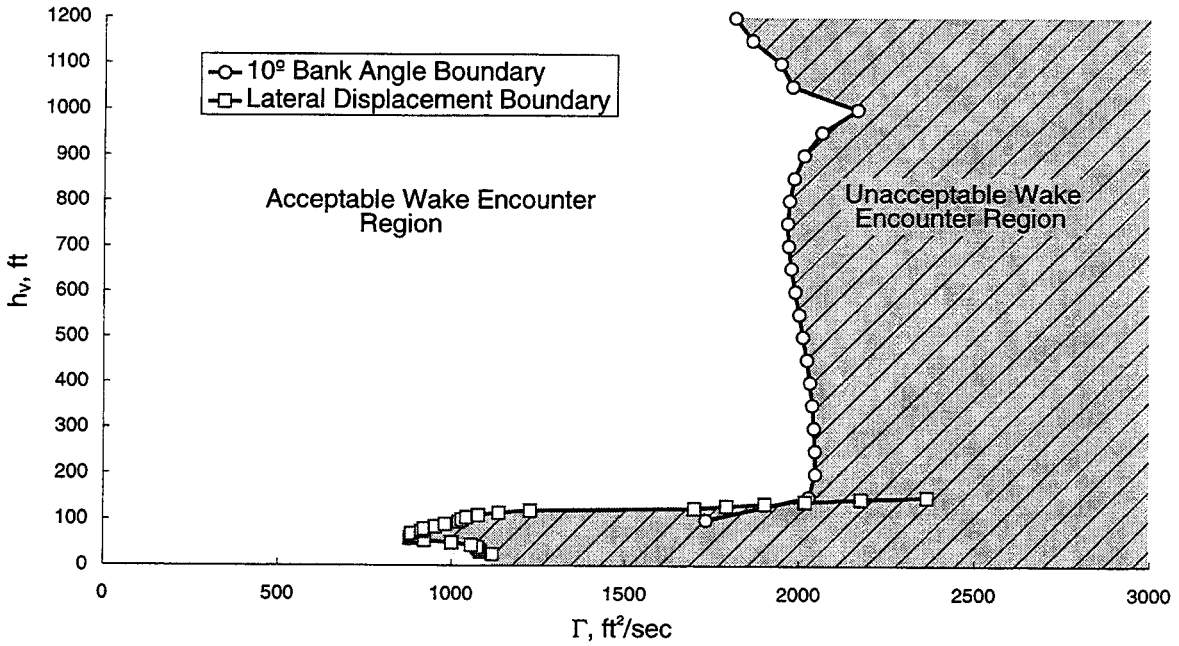


Figure 4. Bank angle and lateral displacement boundary.

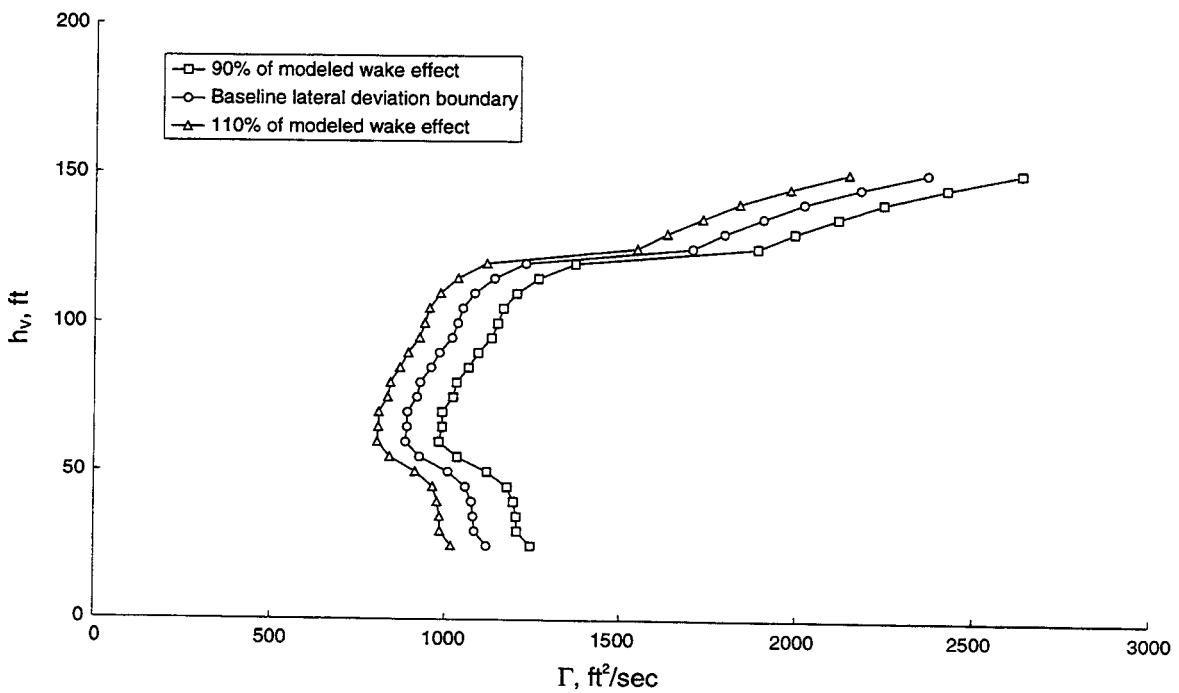


Figure 5. Sensitivity of lateral deviation criteria to mismodeling of wake effect.

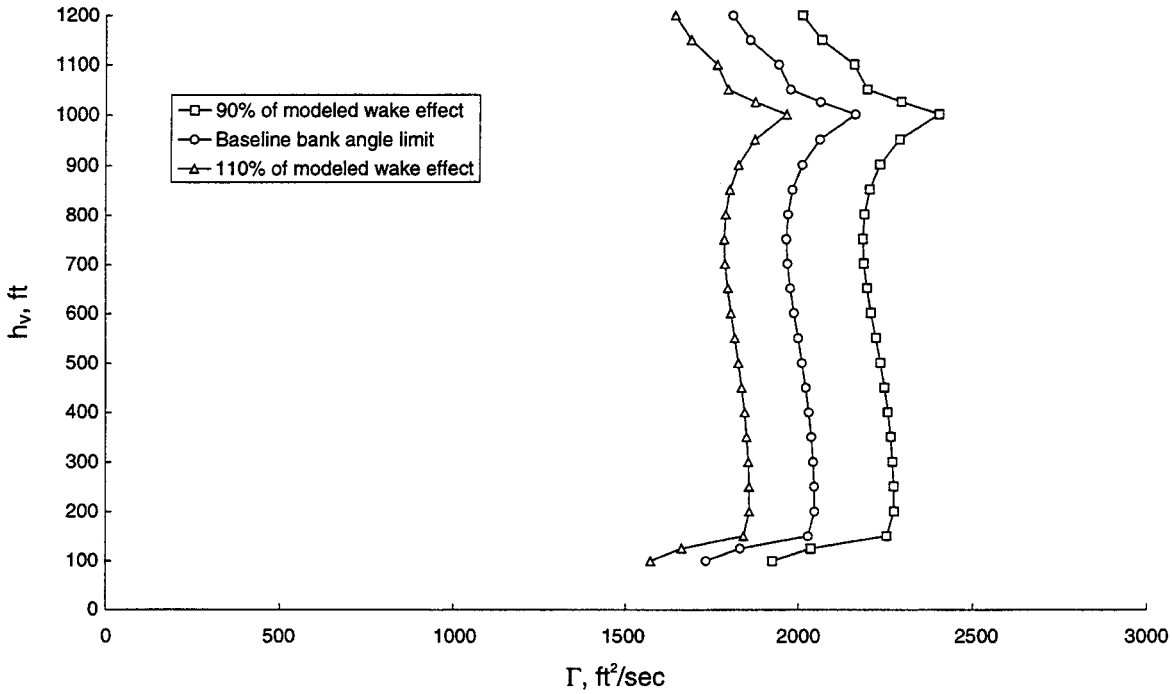


Figure 6. Sensitivity of bank-angle limit boundary to mismodeling of wake effect.